Stem Cell Reports, Volume *15*

Supplemental Information

Transplantation of Skin Precursor-Derived Schwann Cells Yields Better Locomotor Outcomes and Reduces Bladder Pathology in Rats with Chronic Spinal Cord Injury

Peggy Assinck, Joseph S. Sparling, Shaalee Dworski, Greg J. Duncan, Di L. Wu, Jie Liu, Brian K. Kwon, Jeff Biernaskie, Freda D. Miller, and Wolfram Tetzlaff

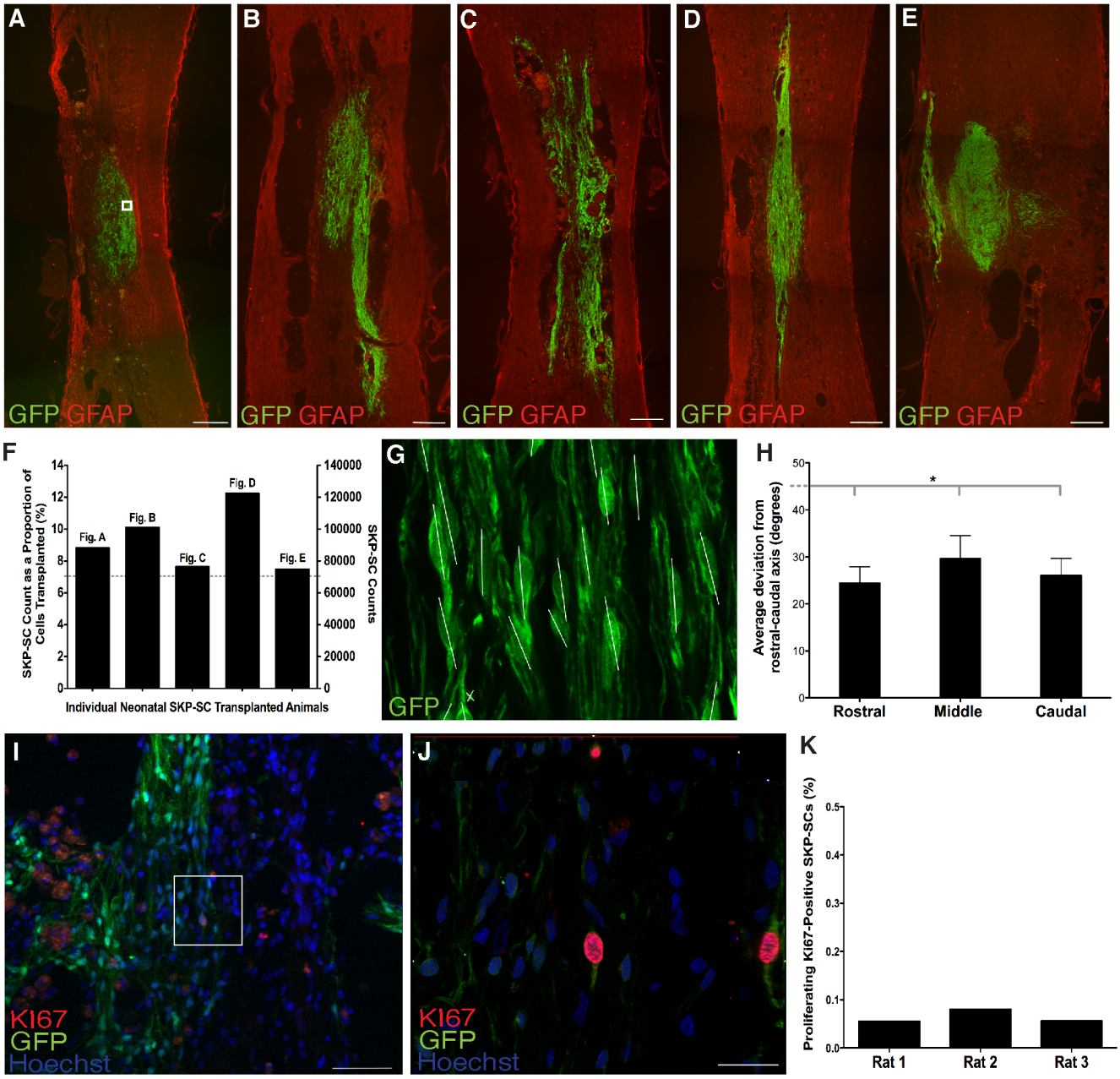
A
B
C
D
E
GFP GFAP
F
SKP-SC Count as a Proportion of Cells Transplanted (%)
SKP-SC Counts
Fig. A
Fig. B
Fig. C
Fig. D
Fig. E
Individual Neonatal SKP-SC Transplanted Animals
G
GFP
H
Average deviation from rostral-caudal axis (degrees)
Rostral
Middle
Caudal
I
KI67
GFP
Hoechst
J
KI67
GFP
Hoechst
K
Proliferating KI67-Positive SKP-SCs (%)
Rat 1
Rat 2
Rat 3

Figure S1. SKP-SCs show a predominantly rostral-caudal orientation and a low incidence of proliferation at 21 weeks post transplantation. Related to Figure 1. (A-E) Photomicrographs of GFAP-immunostained contused spinal cords from the five animals that make up the large transplant SKP-SC 'sub-group' (see Supplemental Experimental Procedures) at 29 wpi used for quantification in Figure S1-3 and axon count analysis (Figure 3). Note that the SKP-SCs integrate into the lesion sites and bridge the cavity. (**F**) SKP-SC counts at 29 wpi for the rats in the large transplant sub-group. Each bar corresponds to the appropriate image shown above (A-E) and is a subset (>70000 cells) of those shown in Figure 1F. **(G)** Photomicrograph of box shown in A demonstrating the associated vectors assigned to each transplanted GFP+ SKP-SC in the orientation analysis. Note that 'x' marks cells that were given a 90-degree value signifying they were coming out of the plane**. (H)** Quantification demonstrating that the majority of transplanted SKP-SCs displayed a strong rostral-caudal orientation at the rostral, middle and caudal regions of the graph as demonstrated by an average deviation from rostral–caudal axis (0 degrees) of 26 degrees. The rostral, middle and caudle deviations were significantly less than 45 degrees (representative of an average random orientation; **p*<0.027; t-test; n=5). **(I)** Photomicrograph demonstrating the low number of transplanted GFP+ SKP-SCs that co-localized with the proliferative marker KI67 at 29 wpi**. (J)** Confocal image taken at the location of the box in I demonstrating clear co-localization of Hoechst and KI67 in the nucleus of a GFP+ SKP-SC. **(K)** To assess proliferation of the transplanted SKP-SC at 29 wpi, we quantified the percentage of GFP+ cells that expressed the marker KI67. Only 0.05% of the cells were KI67+, suggesting minimal proliferation of SKP-SCs at 21 weeks after transplant. This KI67 proliferative index is lower than in benign Schwannomas (average of 1.2% KI67+ cells) and malignant peripheral nerve sheath tumors (average of 23% KI67-positive cells; Ghilusi et al., 2009). Accordingly, there was no indication of SKP-SC derived malignancy in our grafts. Scale bars: 200 μm in A-E, 50 μm in G & I, and 20 μm in J. Data are presented as individual data for F (n=5) and K (n=3) and group means +/- SEM for H (n=5).

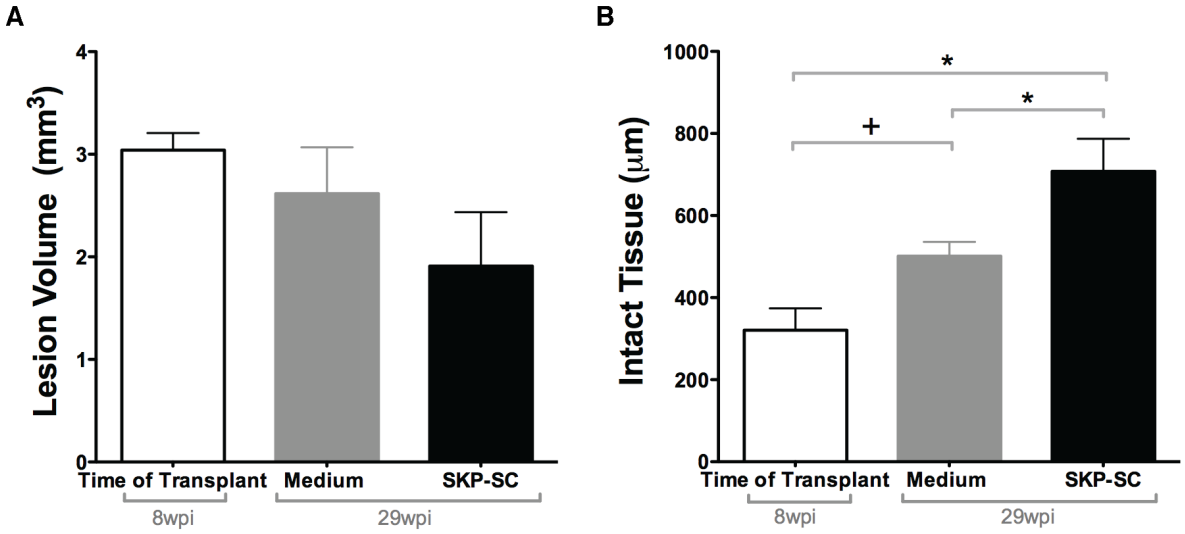

Figure S2. High SKP-SC survival results in more intact tissue than in control animals. Related to Figure 1. **(A)** The mean lesion volume for animals with high transplant cell survival and their appropriate controls is similar among the three groups. **(B)** Mean intact GFAP+ tissue (spared rim and tissue bridges included) showed significant differences among the sub-groups. Note the significantly larger intact tissue in the SKP-SC sub-group with high transplant survival compared to the medium (*p=0.029; ANOVA with LSD) and time of transplant (TofT) control (*p=0.001; ANOVA with LSD) sub-groups. Also, the amount of intact tissue in the medium injected sub-group compared to the TofT control sub-group approached statistical significance (+p=0.051; ANOVA with LSD). Sub-group analysis: SKP-SC n=5; Medium n=5; TofT n=5. All data presented as mean +/- SEM.

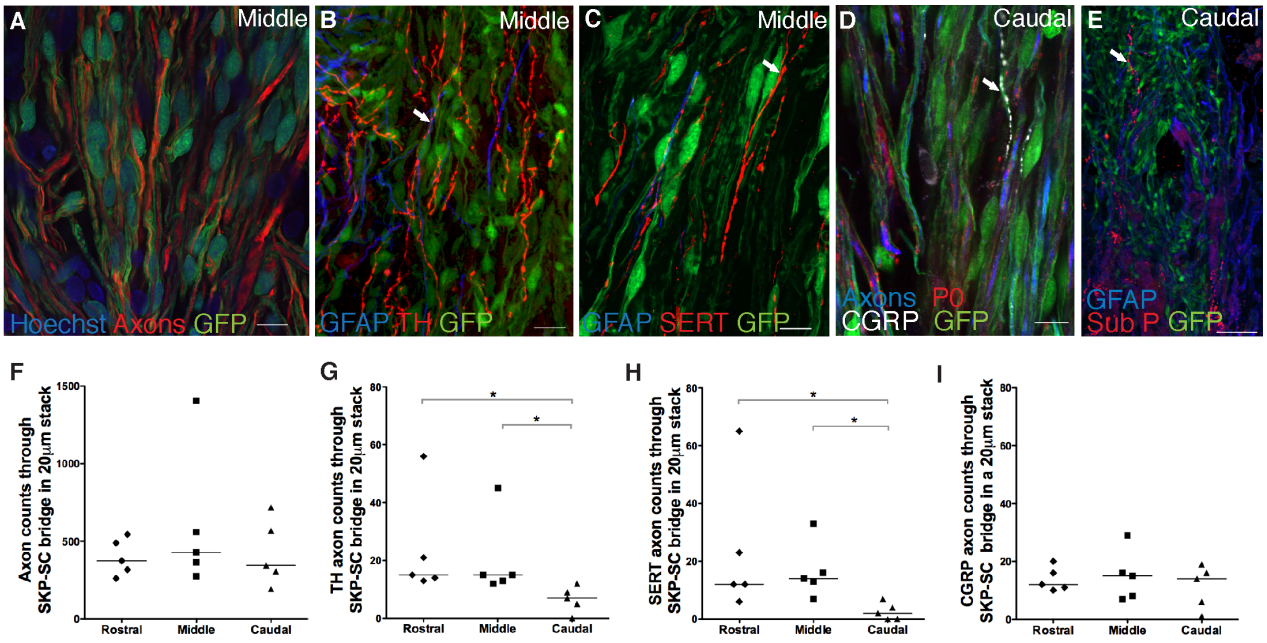

Figure S3. Significantly more TH- and SERT+ axons at the rostral and middle levels of the SKP-SC bridge compared to the caudal levels. Related to Figure 3. Representative photomicrographs depicting NF200/βIII-TUBULIN+ **(A),** TH+ **(B),** SERT+ **(C)**, CGRP+ **(D)**, and Substance P+ **(E)** axons growing through GFP+ SKP-SC bridges. **(F-I)** Quantifications of NF200/βIII-Tubulin+ (F), TH+ (G), SERT+ (H) and CGRP+ (I) axon counts at rostral, middle, and caudal levels (yellow lines in Figure 3E) of the spinal cord in five animals from the SKP-SC sub-group. There were significantly more TH+ and SERT+ axons at the rostral and middle levels of the SKP-SC bridges than at the caudal level (all *p<0.05; Friedman test with follow up Wilcoxon) supporting the interpretation of rostral to caudal regeneration of these brainstem-derived axons. Sub-group analysis: SKP-SC n=5; Medium n=5; TofT n=5. Scale bars: 50 μm for E; 20 μm for B; 10 μm for A,C,D. Individual data points for each animal are presented with group medians indicated by solid black lines in F-I.

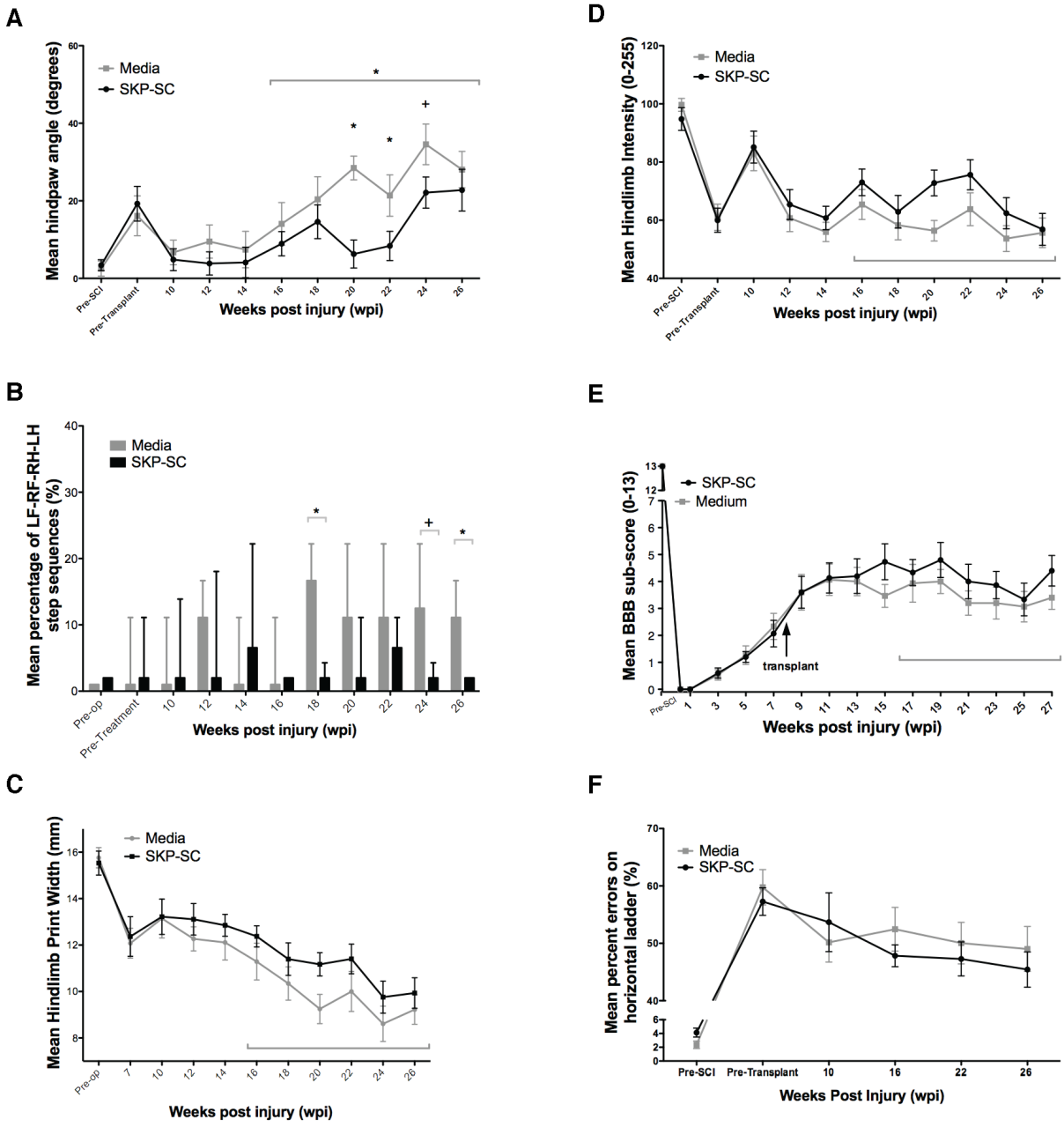

Figure S4. SKP-SCs elicited functional improvements on paw angle and step sequence parameters on the CatWalk. Related to Figure 6. (**A**) SKP-SC transplanted animals showed a significantly lower paw angle (less outward rotation) over the last 10 weeks of behavior, as indicated by a significant interaction (**p*=0.041; repeated measures ANOVA). Follow-up analysis indicated that the SKP-SC group had significantly lower paw angles at 20 and 22 wpi (**p*<0.047; t-test) and a trend at 24 wpi (+*p*=0.072; t-test) but this difference was not maintained at 26 wpi. **(B)** The SKP-SC transplanted group showed a significantly smaller percentage of the abnormal stepping pattern LF-RF-RH-LH as compared to the medium control group at week 18 and 26 (**p*<0.003; MWU) and approached significance at week 24 (+*p*=0.076). There were no significant interactions found on the repeated measures ANOVA in mean hindlimb print width **(C)** or mean hindlimb intensity **(D)** CatWalk parameters or the mean BBB subscore **(E)** or the irregular horizontal ladder **(F).** SKP-SC n=15; Medium n=15. Data is presented as means +/- SEM**.**

Antibody	Source	Concentration
mouse anti-S100β	Sigma-Aldrich, St. Louis, MO **AMAB91038**	1:500
rabbit anti-GFAP	Dako, Glostrup, Denmark **Z0334**	1:1000
goat anti-GFAP	Santa Cruz Biotechnology, Santa Cruz, CA **sc-6170**	1:50
mouse anti-GFAP	Sigma-Aldrich, St. Louis, MO **G3893**	1:500
chicken anti-P0	Aves, Tigard OR **PZ0**	1:100
chicken anti-GFP	Millipore, Billerica, MA **AB16901**	1:1000
rabbit anti-GFP	Millipore, Billerica, MA **AB3080**	1:100
goat anti-GFP	Rockland Immunochemicals, Gilbertsville, PA **600-101-215**	1:200
mouse anti-GFP	Millipore, Billerica, MA **Mab3580**	1:500
mouse anti-neurofilament 200 (NF-200)	Sigma-Aldrich, St. Louis, MO **N0142**	1:500
rabbit anti-NF-200	AbD Serotec, Releigh, NC **AHP245**	1:1000
mouse anti-ßIII-Tubulin	Sigma-Aldrich, St. Louis, MO **T8660**	1:500
rabbit anti-βIII- Tubulin	Covance, Princeton, NJ **PRB-435P**	1:500
rabbit anti-serotonin transporter (SERT)	Immunostar, Hudson, WI **24330**	1:500
sheep anti-tyrosine hydroxylase (TH)	Millipore, Billerica, MA **AB1542**	1:200
rabbit anti-calcitonin gene-related peptide (CGRP)	Sigma-Aldrich, St. Louis, MO **C8198**	1:500
rabbit anti-Substance P	Millipore, Billerica, MA **AB1566**	1:500
mouse anti-P75NTR	Millipore, Billerica, MA **MAB357**	1:500
rabbit anti-laminin	Sigma-Aldrich, St. Louis, MO **L9393**	1:200
mouse anti-neurocan	Developmental Studies Hybridoma Bank, Iowa City, IO; **ID1**	1:100
mouse anti-chondrontin sulfate proteoglycan (CS56)	Sigma-Aldrich, St. Louis, MO **C8035**	1:200
mouse anti-KV1.2 potassium channels	Generous gift from Dr. J. Trimmer, University of California, Davis, CA	1:200
mouse anti-contactin-associated protein (CASPR)	Generous gift from Dr. J. Trimmer, University of California, Davis, CA	1:300
mouse anti-KI67	BD Biosciences, Mississauga, ON **550609**	1:20
Rabbit anti-IBA1	FUJIFILM Wako Pure Chemical Corporation, Osaka Japan; **019-19741**	1:5000

Table S1. List of primary antibodies used. Related to main text Experimental Procedures. Antibody host, source and concentration specific to immunohistochemistry are shown.

Compared Parameters	Correlation Coefficient	P Value
Intact Tissue vs. P0+ve Volume	r=0.502	* p<0.001
Intact Tissue vs. P0+ve Volume Inside Lesion	r=0.429	* p=0.009
Intact Tissue vs. P0+ve Volume Outside Lesion	r=0.557	* p<0.001
Intact Tissue vs. Total Axons	r=0.782	* p=0.001 ϕ
Intact Tissue vs. P75NRT+ve Volume	r=0.388	* p=0.042
Intact Tissue vs. SERT+ Axons	r=0.804	* p=0.000 ϕ
Intact Tissue vs. TH+ Axons	r=0.720	* p=0.004 ϕ
Intact Tissue vs. Lesion Volume	r=-0.469	* p=0.004
P0+ve Volume Outside Lesion vs. 27wpi BBB	ρ =0.648	* p=0.009
P0+ve Volume vs. Total Axons	r=0.492	+ p=0.063 ϕ
P0+ve Volume vs. SERT+ve Axons	r=0.512	+ p=0.051 ϕ
P0+ve Volume vs. TH+ve Axons	r=0.463	+ p=0.080 ϕ
P75NTR+ve Volume vs. SERT+ve Axons	r=0.677	* p=0.031 ϕ
P75NTR+ve Volume vs. TH+ve Axons	r=0.739	* p=0.015 ϕ
BBB 27wpi vs. Ladder % Error 26wpi	ρ =-0.358	+ p=0.052
GFAP Max Value vs. Cavity Volume	r=0.448	* p=0.006
Bladder Wet Weight vs. 27wpi BBB	ρ =-0.501	* p=0.004
Bladder Wet Weight vs 27wpi BBB subscore	ρ =-0.582	* p<0.001

*** Significance p<0.05 + p=0.05-0.1 ϕ Correlations run with sub-groups (n=5).**

Table S2. List of relevant compared significant correlations. Related to Figure 1-6.

Supplemental Experimental Procedures: Related to Experimental Procedures.

Animals

Forty-seven adult female *Sprague Dawley* rats (295±10g; Charles River Laboratories, Wilmington WA) were used in this study. All procedures were approved by the Hospital for Sick Children Research Institute and the University of British Columbia Animal Care Committee in accordance with the guidelines of the Canadian Council on Animal Care. Animals were housed in a room with a reverse light/dark cycle with free access to food and water throughout the study.

Spinal Cord Contusion Injury

Rats received buprenorphine (0.03mg/kg, s.c.) pre-operatively and were anaesthetized with isofluorane (4% induction, ~1.5% maintenance); body temperature was maintained at 36.5±0.5°C. Lidocaine (0.5ml) with 2% epinephrine was injected at the surgical site for additional analgesia and vasoconstriction. The spinal cord was exposed via a thoracic midline incision between T6 and L1 and a laminectomy at vertebra T9 under strictly aseptic conditions. The T8 and T10 dorsal vertebral processes were stabilized with Allen clamps and a 200 Kdyne force-controlled contusion was delivered with an Infinite Horizon (IH) impactor (Precision Systems, Lexington, KY; Scheff et al., 2003). Following injury, muscle and skin were sutured in layers. Lactated Ringers solution (10ml, s.c.) was administered every 12 hours for two days to prevent dehydration. Bladders were manually expressed three times daily until spontaneous micturition returned. Antibiotics (Baytril; 10mg/kg, s.c.) were administered as needed to treat minor bladder infections.

Following injury, three rats were euthanized due to injury-related complications and three rats were excluded from the study prior to treatment, based on spontaneous recovery and injury parameters. We excluded animals that were outliers in terms of injury severity; specifically, we removed animals with the Basso, Beattie, and Bresnahan (BBB) score or subscore at 7 weeks post-injury (wpi) that was >2 standard deviations discrepant from the mean. We also removed animals in which area under the force curve (measured by the Infinite Horizon Impactor) was >2 standard deviations from the mean. Injured rats (n=31) were divided into two groups that were matched based on peak force of injury, area under the force curve, maximum impactor displacement, pre-injury weight, weight prior to transplant, and BBB scores and BBB subscores at 2 days' post-injury and for each subsequent week prior to transplantation. One group was randomly chosen to receive cell treatment (n=15) and the other medium only (n=16) and investigators were blinded to which animals were given either a cell treatment or medium injection. An additional group of rats received the same 200 Kdyne contusion without treatment to form a time of transplant (TofT) control group (n=10); two animals were excluded from this group because the area under the force curve or BBB scores were >2 standard deviations from the pre-treatment group mean used previously.

SKP Isolation and Differentiation into SKP-SCs

As previously described (Biernaskie et al., 2009; Fernandes et al., 2004; Toma et al., 2001; Toma et al., 2005), neonatal primary rat skin-derived precursors (SKPs) were prepared from the back skin of either neonatal (P0-P3) transgenic *Sprague-Dawley* rats that expressed GFP in all cells (SLC, Japan). Secondary spheres were generated by digesting SKPs with collagenase (1mg/ml) then mechanically dissociating to liberate single cells, which were sub-cultured at a density of 35,000-50,000 cells/ml in flasks. Cells were grown at 37ºC and 5% CO_2, fed with SKP proliferation medium (Dulbecco's Modified Eagle's Medium, DMEM:F-12; 3:1; Invitrogen, Carlsbad, CA) containing 1% penicillin/streptomycin (Cambrex, East Rutherford, NJ), 2% B27 supplement (Invitrogen), 20 ng/ml epidermal growth factor (EGF; BD Biosciences, Bedford, MA), and 40 ng/ml fibroblast growth factor 2 (FGF2; BD Biosciences) every 5 days, and passaged every 10 days.

Schwann cells (SC) were differentiated from passage three neonatal SKPs as previously described (Biernaskie et al., 2007; Biernaskie et al., 2006; McKenzie et al., 2006). After two or three passages, purified SKP-SCs were frozen in 90% fetal bovine serum / 10% dimethyl sulfoxide at -80ºC for long-term storage. Approximately 2 weeks prior to transplantation, the SKP-SCs were thawed, plated, and expanded under SC proliferation medium [DMEM/F12 (3:1), 1% penicillin/streptomycin, 2% N2 supplement (Invitrogen), 25 ng/ml neuregulin-1β (R&D Systems, Minneapolis, MN), and 5 μM forskolin (Sigma-Aldrich, St. Louis, MO)]. To investigate the expression of typical SCs markers in the SKP-SC cultures, the cells were fixed for 15 min in 4% paraformaldehyde and stained for GFP, S100B and

Hoechst 33258 (1:1000, Sigma-Aldrich) was used to visualize nuclei. Images were captured via a Zeiss Axiovert 200 spinning disk confocal microscope (Yokogawa, Sugar Land, TX) and C9100-13 EM-CCD camera (Hamamatsu, San Jose, CA), with Volocity acquisition software. SC purity was expressed as the percentage of cells positive for S100β, and the total cell number was determined by Hoechst staining. Four different culture samples were used to determine the purity of neonatal and at least three fields of view were selected randomly (i.e., while visualizing Hoechst) for each sample.

Cell Transplantation

For transplantation at 8 wpi, SKP-SCs were removed from laminin/poly-d-lysine (PDL)-coated plates/flasks by gentle agitation and spraying after 3-5 minute incubation in 0.25% Trypsin/ethylenediaminetetraacetic acid (EDTA). Trypsin was inactivated with 10% fetal bovine serum and cells were triturated gently to produce a single cell suspension, which was then centrifuged (1000 rpm, 5 min.) and re-suspended at 200,000 cells/μl in fresh DMEM:F12 (3:1). Prior to transplantation, rats were anaesthetized and prepared for surgery as outlined above. The laminectomy at T9 was re-exposed and scar tissue was removed to allow access to the site of SCI. One million neonatal SKP-SCs in 5 μl of medium was stereotaxically injected directly into the epicenter of the contusion site using a 10 μl Hamilton syringe fitted with a glass micropipette (~80 μm tip size). Cyclosporine A was delivered to all animals in homecage drinking water (150 mg/l of water; Neoral; Novartis) beginning 4 days before transplantation and continuing for the duration of the study. Oral administration was replaced with injectable cyclosporine A for 4 days post-transplantation (Sandimmune, Novartis; 15mg/kg, s.c.). One medium injected animal was euthanized in the 5 days following the transplantation surgery due to bladder complications (final n=15).

Behavioural Assessments

All behavioral raters were blind to the treatment groups. Functional locomotor abilities were assessed bi-weekly using the open-field BBB score and subscore; (Basso, 2004; Basso et al., 1995), footprint analysis (CatWalk, Noldus, Netherlands; (Hamers et al., 2001), and the irregular horizontal ladder (Metz and Whishaw, 2002). All animals were acclimatized to the testing environment/equipment and trained prior to collection of baseline behavioural data, which were collected during the week prior to SCI. The animals were given two days to recover from SCI before open field-testing resumed, and seven weeks to regain consistent weight supported stepping prior to resuming Catwalk and ladder testing. Animals were further acclimatized to CatWalk and ladder apparatuses prior to the collection of 7 wpi pre-treatment baseline data. The animals were given one week to recover from transplantation surgery before open field-testing resumed and two weeks before CatWalk and ladder testing resumed. From that point onward, all locomotor tests were conducted bi-weekly at the same time of day by the same investigator until 27 wpi.

Open Field Locomotion (BBB).
Open field locomotion was scored on the BBB scale (Basso et al., 1995), and BBB subscale (Basso, 2004). Two raters assigned a score at the time of testing and all animals scored a 21 on the BBB and a 13 on the BBB subscore during pre-injury baseline assessments.

CatWalk.
The CatWalk system (Noldus, Netherlands), enables objective assessment of locomotion parameters based on quantitative footprint data (Hamers et al., 2001; Vrinten and Hamers, 2003). Unusable runs were identified based on the following criteria: 1) running at an inconsistent speed, 2) stopping in the middle of the run, 3) running exceptionally fast or slow. At least five runs were recorded for each rat during each testing session, and three runs were selected by a rater based on consistency of the run and the inclusion of three complete uninterrupted step cycles. The following parameters were examined: forelimb and hindlimb stride length, hindlimb paw angle, hindlimb paw width, hindlimb paw print intensity, and overall step sequence patterns. CatWalk footprint analysis assessing forelimb and hindlimb stride length was normalized to pre-transplant values.

Irregular Horizontal Ladder.
Hindlimb stepping was also assessed using the irregular horizontal ladder (Metz and Whishaw, 2002). Animals were trained to cross the ladder toward their home cage and each crossing was recorded using a high definition digital camera (Sony, Toronto, Canada) for subsequent scoring. The ladder always included the same number of overall rungs and spaces (ranging from one-five missing rungs per space), but the rung positions were changed for each

testing session to avoid any training effects. A frame-by-frame analysis of video recordings of hindlimb stepping yielded error scores (averaged over five trials per session per animal) for the number of overall steps and errors for each hind paw (Metz and Whishaw, 2002).

Tissue Processing

Prior to euthanasia and transcardial perfusion, the bladder of each rat was emptied by manual expression. The TofT control group was euthanized at 8 wpi, whereas the SKP-SC- and medium-treated rats were euthanized at 29 wpi. All rats were overdosed with ketamine (210 mg/kg, i.p.) and xylazine (30 mg/kg, i.p.) and transcardially perfused with 0.12M PBS followed by 4% paraformaldehyde in PBS (0.1M). The thoracic spinal cord encompassing the injury site and the bladder were removed, post-fixed overnight in 4% paraformaldehyde, cryoprotected overnight in 12, 18, and then 24% sucrose in 0.12M PBS, frozen on dry ice and stored frozen at -80°C. The thoracic spinal cord was sectioned longitudinally in the sagittal plane with 10 sets of slides with each slide containing 10 spinal cord sections 200 μm from dorsal to ventral. The bladder was sectioned transversely twice 200 μm apart through the midline. Generally, the central canal was used to determine the center section (mid-sagittal plane) to align equal tissue on both sides for analysis. Both the spinal cord and bladder sections were cut at a thickness of 20 μm using a Microm cryostat (Heidelberg, Germany) onto Superfrost Plus slides (Fisher, Houston, TX) and stored at -80°C.

Immunohistochemistry

Tissue sections were permeabilized with 0.1% Triton-X-100 and treated with 10% donkey serum for 30 min to prevent non-specific binding. For immunolabeling of myelin proteins, brief delipidation was also performed, using graded ethanol solutions prior to the blocking step. For a list of the primary antibodies used, see Table S1. The secondary antibodies were generated in donkey or goat, conjugated with Dylight fluorochromes 405, 488, 594 or 649, and used at a concentration of 1:200 (Jackson ImmunoResearch Laboratories, West Grove, PA). Nuclei were stained with Hoechst 33342 (1:5000).

Histological Quantifications

A Zeiss (Oberkochen, Germany) Axioplan 2 microscope fitted with image acquisition software (Northern Eclipse; Empix, Mississauga, Canada) was used for low magnification images. For higher magnification images, including those used for cell counts, axon counts, and confirmation of co-localization, images were captured on a Zeiss AxioObserver Z1 (Zeiss, Germany) confocal microscope fitted with a CSU-X1 Yokogawa spinning disc and solid-state lasers with 405, 488, 565 and 639 wavelengths. All image analysis was completed by individuals blind to treatment. Associated with this, the green channel (with GFP+ cells) was not provided to the individuals assessing histological outcomes except when necessary; e.g., for GFP+ cell counts and GFP+ volume analyses. Images were merged using Photoshop CS2 or CS4 (Adobe, San Jose, CA). All measurements (e.g., distances, areas, and intensities) except cell/axon counts and vector analysis were performed with Sigma Scan Pro 5 (Systat, Chicago, IL).

Among SKP-SC-treated rats, we defined a sub-group of five animals with very successful survival of transplanted cells (defined by more than 70,000 cells present; see Figure 1F; Figure S1) and compared them to a matched (by injury force/displacement and pre-transplant behavioral parameters) medium-treated sub-group (n=5) and a matched TofT sub-group (n=5). This sub-group analysis was conducted to see whether long-term survival of grafted cells is required for specific observed benefits (e.g., lesion volume and intact tissue width; Figure S2) or when performing counts on all 38 animals was not practical (axon and axon sub-type counts: Figure 3G-I, Figure S3; SKP-SC orientation analysis: Figure S1).

Determining Lesion Volume, Average Intact Tissue, and Tissue Width.
All three analyses were completed using all longitudinal spinal cord tissue sections (200 μm apart) and the central canal was used to align the spinal cord sections. Tissue was processed with antibodies to GFAP (reactive astrocyte marker) prior to imaging at 5X. Lesion area was defined as GFAP-negative area or GFAP+ area with disrupted/abnormal cytoarchitecture and was manually outlined in each spinal cord section. Cavalieri's principle was applied for volume calculations, i.e., $V = \Sigma$ [area x section thickness x number of sections in each sampling block]. The same sections were used to estimate the amount of intact tissue; we measured the thinnest combination of both 1) the spared rim representing the narrowest width of the rim with GFAP+ tissue with normal

cytoarchitecture on either side of the lesion (as described above); 2) any additional normal-appearing cytoarchitecture resulting from spared tissue bridges. The narrowest width of spared tissue was summed within a section and the average sum from all sections of one animal yielded the mean intact tissue value for that animal.

SKP-SC Transplant Volumes, Transplant Counts, Orientation and Proliferation.
Transplant volumes were completed using all longitudinal spinal cord tissue sections (200 μm apart) with the central canal being used to align the spinal cords and processed with antibodies against GFP, P0, and GFAP. Images were taken at 5X and thresholds were set by the observer to yield an area occupied by the GFP+ SKP-SCs using Sigma Scan software. These GFP+ transplant areas were further subdivided into regions inside the lesion (defined above) versus outside the lesion and converted into transplant volumes using Cavalieri's principle.

The high-survival transplant sub-group (n=5) was used to estimate densities of the SKP-SCs within these transplants. To obtain GFP+ cell counts, sections every 400μm through the entire spinal cord were imaged (n=5) and optical dissector boxes (100μm^2) were randomly placed at a distance of 320um from one another throughout sections containing GFP+ grafts. Confocal Z-stacks were imaged (at 63x) if they contained GFP+ cells and GFP+/Hoechst+ SKP-SCs were counted within the volume of the z-stacks using the optical dissector technique (West M.J. (2012) Basic Stereology for Biologists and Neuroscientists. Cold Spring Harbor, New York: Cold Spring Harbor Laboratory Press). This method is well-established as an accurate way to obtain an average transplant cell density. The resulting GFP+ SKP-SC density was used to estimate the total number of SKP-SCs in the previously measured GFP+ volumes in SKP-SC-treated animals. The volume of SKP-SCs ranged from 0.0006 to 0.23 mm^3 and the average density of cells was $5.325x10^{-4}$ cells/μm^3. In the same set of images, we determined the percentage of GFP+ SKP-SCs that were also P0+, to yield the percentage of myelinating SKP-SCs.

The average orientation of the transplanted SKP-SCs was measured in the SKP-SC sub-group (n=5): three serial sections were selected and single plane images of the GFP+ area were analyzed with ImageJ software (National Institute for Health, USA). Each cell was assigned a vector representing the orientation of the cell and the deviation away from zero (rostral-caudal orientation) was calculated and compared between the rostral, middle and caudal sections of the cord. Cells that were observed in cross section (i.e. orthogonal to the plane of sections) were given a 90° value. The orientation values were compared to a value of 45 degrees (representing a random orientation of the cells in a 2D plane).

An additional quantification of SKP-SC proliferation was performed in three animals (with transplantation estimates >70,000 cells), by counting the GFP+ cells that co-expressed the proliferation marker KI67 at 21 wpi.

GFAP Intensity Analysis.
Analyses was completed using all longitudinal spinal cord tissue sections (200 μm apart) with central canal used to align cords. Intensity profiles of the GFAP immunoreactivity were generated along six (one pixel wide and 320 μm long; 5X primary magnification; Figure 2A-C) lines perpendicular to the lesion edge. The animal averages were then averaged for each group and further broken down according to whether or not this drawn line (extended into the lesion) was directly on SKP-SCs (GFP+), directly on endogenous SCs (GFP-negative, P0+) or directly on cavity (with no SKP-SCs or P0+ endogenous SCs in the vicinity). In each situation, the intensity data was normalized to the far distant rostral intact cord for each given animal to correct for inter-animal variations.

SC Myelination and Non-myelinating SC Analysis.
Analyses was completed using all longitudinal spinal cord tissue sections (200 μm apart) with central canal used to align cords. The overall volume of SC myelin (P0+) was measured using a thresholding procedure as described for the GFP+ transplant volume in 5X images. The volume of P0+ myelin associated with transplant-derived SKP-SCs was estimated by measuring the overlap between GFP+ and P0+ areas on each section and converting those areas to volumes (as described above). All P0+ structures not closely associated with GFP+ SKP-SCs were assumed to be of endogenous SC origin. The myelination state was corroborated with antibodies, including CASPR and the voltage gated potassium channel KV1.2., known markers surrounding the nodes of Ranvier. To examine the non-myelinating SC content of the 29 wpi spinal cord tissue, we used P75NTR immunohistochemistry and conducted a volume estimate using the same methods as for GFP+ and P0+ volume analyses described above on an adjacent set of sections.

Axon Counts.
Two axon analyses were conducted in the three sub-groups (n=5 each). In the first analysis comparing the transplantation groups, for each animal, we counted the number of axons in a single 63X optical plane in five sections spaced 200μm apart, whereby the middle section contained the central canal. Axons were counted when crossing a line spanning the lesion (as defined previously) at the narrowest point of the spinal cord (blue lines; Figure 3A,C,E). In addition, we counted the number of axons, axon subsets, and/or P0+ myelinated axons within the GFP+ SKP-SC bridges at three lines drawn at the rostral (100μm from rostral interface), middle, and caudal (100μm from caudal interface) portions of the GFP+ grafts (yellow lines; Figure 3E) to further determine whether any gradients of axon growth exist, e.g. due to ingrowing supraspinal axons. Axons that intersected with the drawn lines were counted throughout the single 20 μm section using the section with the largest SKP-SC transplant area which happened to be within 200 μm ventral to the central canal. Images for all axon counts were captured at 63X, including TH+ axons, SERT+ axons, CGRP+ axons, axons (βIII tubulin/NF-200), and P0+ axons (βIII tubulin/NF-200/P0+). Axons surrounded by P0+ sheaths were counted to calculate the percentage of myelinated axons within the SKP-SC bridges.

Bladder Analysis.
Wet weight of the dissected bladders was recorded. Bladders were then dabbed dry and a small 3 mm ring-shaped band was cut from the bladder starting at the rostro-caudal midline moving caudally and frozen in Tissue-Tek O.C.T. (Sakura, Netherlands) in an orientation that allowed for transverse sectioning of the bladder wall. Bladders were handled carefully in dissection and preparation to avoid stretching the tissue; also, tissue preparation was performed by blinded experimenters. Four animals were excluded from the bladder analysis due to severe damage to the bladder during tissue processing. Sections were stained for 5 minutes in 0.1% Cresyl Violet and subsequently imaged at 10X. Two sections were measured per animal (2000μm apart), where a one-pixel thick line was drawn through the thickest section of the bladder wall to obtain a mean max wall thickness.

Statistical Analyses

Statistics were calculated using SPSS (IBM; Markam ON, CA). If data met assumptions of normality and homogeneity of variance, groups were compared using the appropriate independent t-test, paired t-test, or a repeated measures (RM) analysis of variance (ANOVA) for two groups and using a one-way ANOVA with a Least Significant Difference *post hoc* test for three groups with data presented as mean ± SEM. If the assumptions of normality and homogeneity of variance were not met: groups were compared using the Kruskal-Wallis (KW) one-way analysis of variance with follow up Mann-Whitney U (MWU)-test for three independent groups and just the Mann-Whitney U-test for two paired groups or a Friedman test with follow up Wilcoxon test for three paired groups and just the Wilcoxon test for two paired groups with data presented as raw values with the median indicated. Correlation analysis was conducted using Pearson's correlation coefficient (parametric) or Spearman's rank correlation coefficient tests (non-parametric). The significance level for all two-tailed tests was $p<0.05$. Trends were reported for two-tailed tests when $p<0.1$ indicative of a significant one-tailed test.

Supplemental References:

Basso, D.M. (2004). Behavioral testing after spinal cord injury: congruities, complexities, and controversies. J Neurotrauma *21*, 395-404.

Basso, D.M., Beattie, M.S., and Bresnahan, J.C. (1995). A sensitive and reliable locomotor rating scale for open field testing in rats. J Neurotrauma *12*, 1-21.

Biernaskie, J., Paris, M., Morozova, O., Fagan, B.M., Marra, M., Pevny, L., and Miller, F.D. (2009). SKPs derive from hair follicle precursors and exhibit properties of adult dermal stem cells. Cell Stem Cell *5*, 610-623.

Fernandes, K.J., McKenzie, I.A., Mill, P., Smith, K.M., Akhavan, M., Barnabe-Heider, F., Biernaskie, J., Junek, A., Kobayashi, N.R., Toma, J.G*., et al.* (2004). A dermal niche for multipotent adult skin-derived precursor cells. Nat Cell Biol *6*, 1082-1093.

Ghilusi, M., Plesea, I.E., Comanescu, M., Enache, S.D., and Bogdan, F. (2009). Preliminary study regarding the utility of certain immunohistochemical markers in diagnosing neurofibromas and schwannomas. Rom J Morphol Embryol *50*, 195-202.

Hamers, F.P., Lankhorst, A.J., van Laar, T.J., Veldhuis, W.B., and Gispen, W.H. (2001). Automated quantitative gait analysis during overground locomotion in the rat: its application to spinal cord contusion and transection injuries. J Neurotrauma *18*, 187-201.

McKenzie, I.A., Biernaskie, J., Toma, J.G., Midha, R., and Miller, F.D. (2006). Skin-derived precursors generate myelinating Schwann cells for the injured and dysmyelinated nervous system. J Neurosci *26*, 6651-6660.

Metz, G.A., and Whishaw, I.Q. (2002). Cortical and subcortical lesions impair skilled walking in the ladder rung walking test: a new task to evaluate fore- and hindlimb stepping, placing, and co-ordination. J Neurosci Methods *115*, 169-179.

Scheff, S.W., Rabchevsky, A.G., Fugaccia, I., Main, J.A., and Lumpp, J.E., Jr. (2003). Experimental modeling of spinal cord injury: characterization of a force-defined injury device. J Neurotrauma *20*, 179-193.

Toma, J.G., McKenzie, I.A., Bagli, D., and Miller, F.D. (2005). Isolation and characterization of multipotent skin-derived precursors from human skin. Stem Cells *23*, 727-737.

Vrinten, D.H., and Hamers, F.F. (2003). 'CatWalk' automated quantitative gait analysis as a novel method to assess mechanical allodynia in the rat; a comparison with von Frey testing. Pain *102*, 203-209.